Copyrighted Materials
Copyright © 2010 SciTech Publishing Retrieved from www.knovel.com

CHAPTER 3

Radar Search and Overview of Detection in Interference

James A. Scheer

Chapter Outline

3.1 INTRODUCTION

Though radar systems have many specific applications, radars perform three general functions, with all the specific applications falling into one or more of these general functions. The three primary functions are *search*, *track*, and *image*. The radar search mode implies the process of target detection. Target tracking implies that the radar makes measurements of the target state in range, azimuth angle, elevation angle, and Doppler frequency offset. This is not to exclude the fact that a search radar will perform target measurements to provide a cue for another sensor, for example, or that a track radar will perform the detection process.

Many tracking radar systems track a single target by continually pointing the antenna beam at the target and controlling the antenna pointing angle and range measurement to coincide with the target position. The tracking function is performed by a set of analog circuits controlling the antenna and range servo. In many modern systems, though, the tracking function is performed by processing a sequence of target state measurements made by the tracking sensor (radar). These measurements are applied to a computer algorithm that forms a target track file. The tracking algorithms, usually implemented in software, develop an accurate state vector (position, velocity, and acceleration) for the target, typically in a Cartesian coordinate system of North, East, and down. That state estimate then becomes an integral part of a fire control system, directing a weapon or cueing another sensor to the target state.

Once a target is detected and in track, depending on the application for the radar, an imaging mode may be implemented that develops high-resolution data in range, azimuth,

elevation, and sometimes Doppler.[1] This would support target classification, discrimination, and or identification functions. The present chapter is designed to provide the detailed description of the radar processes associated with supporting the search and detect functions. Sensor measurements are covered in Chapter 18, the track function is described in Chapter 19, and the two-dimensional (2-D) imaging function is described in Chapters 20 and 21.

Some systems are designed to perform two or three of these tasks. One way to do this is with multiple radar systems: one optimized for search and another for track. In many cases, however, allowable space and prime power limitations do not allow for multiple radar systems. If a single radar system has to perform both the search function and the track function, then there is likely a compromise required in the design. The following sections will show that some of the features of a good search radar will not be desirable in a good track radar. These same features do not necessarily necessitate a compromise in the imaging mode, however.

The single-pulse signal-to-noise ratio (SNR) can be predicted by exercising the peak power form of the radar range equation (RRE). Seldom, if ever, is a target detected on the basis of a single pulse. Usually there is an opportunity to process several pulses while the antenna beam is pointed at a target. As presented in Chapter 2, this leads to the development of the average power form, or "energy" form, of the RRE, for which the SNR is determined by average power and *dwell time,* T_d. In this case, the dwell time is the time it takes to transmit (and receive) the n pulses used for detection. If these pulses are processed coherently using coherent integration or, more often, fast Fourier transform (FFT) processing, the time duration is often called the *coherent processing interval* (CPI). "CPI" and "dwell time" are often used synonymously. Since not all radar systems are coherent, it is not necessary that coherent processing is performed during a processing interval. The processing may be noncoherent, or the resulting signal may simply be displayed on the radar display.

As an antenna beam is scanned in angle over a designated volume in search of a target, the beam is often pointed in a given angular direction for a time that is longer than the dwell time or CPI. An electronically scanned antenna (ESA) can be pointed at a given angle for an arbitrary time, as determined (directed) by the resource management algorithms implemented in the radar processor. A mechanically scanned antenna will be pointed at a given angular point in space for the time it takes for the antenna beam to scan one half-power beamwidth (θ_3 or ϕ_3) when scanning at an angular rate of ω radians per second. It is not uncommon for the antenna to be pointed at a point for 10 CPIs, for example. To differentiate the antenna scanning dwell time from the coherent processing interval, the term *antenna dwell time*, T_{ad}, to represent this time will be adopted.

The antenna dwell time for a mechanically scanned antenna is found from

$$T_{ad} = \frac{\theta_3}{\omega} \tag{3.1}$$

and the number of CPIs, n_{CPI}, that occur during that time is

$$n_{CPI} = \frac{T_{ad}}{T_d} = \frac{\theta_3}{\omega T_d} \tag{3.2}$$

[1]Radars whose primary function is imaging generally do not have search-and-track modes. Some new systems combine imaging with detection and tracking of targets within the image.

The CPI dwell time, T_d, depends on the radar pulse repetition frequency (PRF) or the pulse repetition interval (PRI) and the number of pulses in a CPI, n, and is given by

$$T_d = nPRI = \frac{n}{PRF} \tag{3.3}$$

To demonstrate by example, a mechanically scanned antenna with a beamwidth of 50 mrad (about 3 degrees) scanning at a rate of 90 degrees per second (about 1.55 radians per second) will produce an antenna dwell time, T_{ad}, of about 33 milliseconds. If a radar has a 10 kHz PRF and transmits 32 pulses for a coherent processing interval, then the CPI, or T_d, is 3.2 milliseconds. There is an opportunity for up to 10 CPIs to be processed in a single antenna dwell.

Dwell time, T_d, and CPI are terms that occur regularly in the literature, whereas the term antenna dwell time, T_{ad}, does not. The use of the variable T_{ad} provides a way to unambiguously differentiate between the antenna dwell time and a signal-processing dwell time.

This chapter discusses how a radar performs a volume search, given a limited instantaneous field of view determined by the antenna beamwidth; the fundamental analysis required to relate SNR to probability of detection, P_D, and probability of false alarm, P_{FA}; and the reasons for using more than one dwell time at each beam position. It will be determined whether it is more efficient to dwell for multiple dwell periods or to use extended dwell times within a CPI for equivalent detection performance. Initially, receiver thermal noise will represent the interfering signal. This will be followed by a discussion of jamming noise and then clutter as the interfering signal.

3.2 SEARCH MODE FUNDAMENTALS

A search radar is designed to look for targets when and where there is no a priori knowledge of the target existence. It is designed to search for a given target type in a given solid angle volume out to a given slant range in a specified amount of time. These parameters are derived from the system application requirements. As an analogy, the situation is much like a prison searchlight illuminating a prison yard, looking for prisoners trying to escape over the fence. The light must scan the area in a time short enough that a prisoner can't run from the building to the fence and escape between searchlight scans. The following several sections will develop the methodology to determine radar requirements for a given search requirement.

It is important to realize that use of an ESA beam (phased array) and a mechanically scanned antenna beam lead to somewhat different search patterns. The mechanically scanned beam scans in one angular dimension over some period of time. For a system designed to search a full 360 degree azimuth sector, the antenna continually rotates in one direction. This is typical of a ground-based weather radar, an air traffic control radar, and a ship-based volume search radar, searching for threats over a full hemisphere. For a system that has to search a limited azimuth sector, such as a 90 degree sector centered in a given direction, the antenna scans in one azimuth direction and at the end of the designated sector will turn around to scan in the other direction. This is typical of an airborne interceptor system, such as an F-15, F-18, or F-22 aircraft radar. A forward-looking airborne commercial weather radar would have a similar scan pattern. In any case, for the mechanically scanned antenna the scanning motion is continuous and smoothly transitions from one beam position to the next, as the radar system performs the detection process; for an electronically scanned antenna, the beam positions will be changed incrementally.

Many modern radar systems employ phased array antenna technology, providing an ability to scan the antenna beam position electronically. An ESA beam can step incrementally from one position to the next in discrete angular steps. Since there are no limits associated with inertia, motor drives, or mechanical reliability, these time-sequential antenna pointing positions do not need to be contiguous in space. In fact, they can be somewhat arbitrary, dictated by the system requirements. For example, a radar using an ESA can search a volume, and interleaved with the search function it can track one or more targets. This is typical operation for a weapons locating radar such as the U.S. Firefinder system, which is designed to search a volume just above the horizon and to track detected artillery and mortar rounds. Legacy Naval surface ship-tracking systems were designed to track only one target, so if multiple targets had to be tracked, a separate tracking radar would be necessary for each target. These systems are currently still in service; however, the next generation of surface ships will have a phased array multifunction radar system, which will reduce the number of radars on the superstructure.

3.2.1 Search Volume

A search radar is designed to search a solid angle volume within a given time. The volume may be as small as a few degree elevation sector over a limited (e.g., 90°) azimuth sector. An example of a small search volume is the AN/TPQ-36 and AN/TPQ-37 Firefinder radars. They are designed to search just above the horizon over a 90° azimuth sector, looking for mortar and artillery rounds out to about 30 km range. If artillery rounds are detected, then the radar tracks them long enough to estimate the point of launch so that counterfire can be issued. The Firefinder is a phased array radar, so the search-and-track functions are interleaved. The search function is not interrupted for long periods of time. Another example of a limited search volume is a ship self-defense system, in which the radar is looking for incoming cruise missiles over all azimuth angles but only at elevations at or near the sea surface. The search volume for these relatively narrow elevation sectors is often referred to as a search *fence*, referring to the general shape of the search pattern.

Some search radars are designed to search a much larger volume, up to a full hemisphere (2π steradians of solid angle). This might be the case for radars searching for incoming ballistic missiles or high-flying anti-ship missiles. In this case, it is expected that the time allowed to complete a single complete search pattern would be longer than that for a Firefinder-like or ship self-defense application.

3.2.2 Total Search Time

For an ESA, the total frame search time, T_{fs}, for a given volume is determined by the number of beam-pointing positions, m, required to see the entire search volume contiguously and by the antenna dwell time, T_{ad}, required at each beam position to achieve the detection range required:

$$T_{fs} = mT_{ad} \tag{3.4}$$

The number of beam positions depends on the total solid angle to be searched, Ω, and the product of the azimuth and elevation beamwidths, θ_3 and ϕ_3. Assuming that the beam positions are contiguous and not overlapping in angle:

$$m = \frac{\Omega}{\theta_3 \phi_3} \tag{3.5}$$

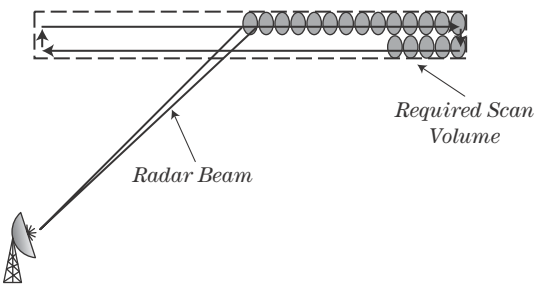

FIGURE 3-1 ■ ESA radar antenna beam scanning in the search mode.

For example, if the search volume is a sector covering 90° in azimuth and 4° in elevation and the azimuth and elevation beamwidths are both 2°, then there will be 45 beam positions in azimuth and 2 beam positions in elevation, resulting in 90 total beam positions. Figure 3-1 depicts a sequence of discrete beam positions designed to cover a specific scan volume having two rows. Note that for clarity not every beam position is depicted.

Combining equations (3.4) and (3.5), the total frame scan time, T_{fs}, is

$$T_{fs} = \frac{\Omega T_{ad}}{\theta_3 \phi_3} \tag{3.6}$$

If the antenna beam dwells at each beam position for 10 msec, then the total scan time for the 90 beam positions is 900 msec. This time ignores the time it takes for the beam to move from one position to the next, which, for a modern electronically scanned antenna, is usually short relative to the antenna dwell time. During the 10 msec antenna dwell time, there might be several CPIs. For example, if the system has a PRF of 20 kHz and 40 pulses are transmitted during a single CPI, then a single CPI, or T_d, would be 2 msec, and each beam position would have five CPIs.

In this example, antenna beams would be spaced at the –3 dB point on the beam (−6 dB round trip) which would produce a *beamshape loss*, or *scalloping loss*,[2] because the target would not necessarily be at the peak of the beam at detection. One way to reduce this loss is to reduce the beam spacing, thus increasing the number of beam positions.

For a mechanically scanned antenna, the scan rate is determined by the total angular search time and the total angle required. The antenna dwell time can be no longer than the time it takes the beam to scan past a given position and must be consistent with the detection performance in the same way as for the ESA. If, for example, the 2° beam has to be at each of the 45 beam positions for 10 msec, then the time for the beam to scan the 90 degree azimuth sector is 450 msec. The scan rate, ω, would be 90 degrees per 450 msec, or 200 degrees per second.

3.2.3 Phased Array Antenna Issues

When using an electronically scanned antenna for performing the search operation, the beamwidth and gain change with scan angle.[3] This change in beamwidth and gain must be considered in designing the search program. As the beam is scanned away from normal

[2]This effect is often called *straddle loss* in range and Doppler processing.

[3]See Chapter 9 for a more detailed discussion of these effects.

to the plane of the aperture, the antenna gain reduces because of two effects. The first is that the effective aperture (i.e., the projection of the antenna surface area in the direction of the beam scan) is reduced by the *cosine* of the scan angle. For a modest scan of, say, 10 degrees, this effect is mild. However, for a 45 degree scan angle the cosine is 0.707, resulting in a gain reduction of about 1.5 dB. For a fixed dwell time, this results in an SNR reduction of 3 dB, because the gain is squared in the radar range equation.

The second effect that reduces the antenna gain is related to each of the radiating elements in the antenna having its own beam pattern, which is at its peak broadside to the aperture but falls off with scan angle. For small scan angles this again represents a marginal reduction in gain, though for large scan angles it can be significant. This loss adds to the effective aperture loss.

The consequence of this scan loss is that the detection performance will degrade as the scan angle increases. Target detection performance is usually required to be equally good at all scan angles. If a system is designed such that it achieves the required performance at the largest scan angle, where the losses are greatest, it will perform well beyond the requirements at a small scan angle. One way to normalize performance at all scan angles is to lengthen the processing time (dwell time) at large angles and to shorten it at small scan angles to counteract the antenna gain variations. This is usually done in quantum steps. For example, a system might have a dwell time of T_d at scan angles of 0 to 15 degrees, $2T_d$ at 15 to 30 degrees, and $4T_d$ at 30 to 45 degrees. The ESA technology allows this adaptation. Mechanically scanned antennas do not experience this gain change with scan angle, so they do not have to adapt the dwell time.

In the search mode, as described in Chapter 2, the beamshape loss usually has to be accounted for since the target may be at any arbitrary angle in the beam when detection is attempted. In addition to the gain loss, the beamwidth widens as the electronically scanned beam is scanned away from normal due to the reduced effective aperture. This widening partially offsets the effect of gain loss, because the beamshape loss is reduced. The designer can take advantage of this reduced loss by decreasing the dwell time at off-normal beam positions or by increasing the antenna beam step size. Increasing the step size maintains a constant beamshape loss. In the target tracking mode, the antenna beam can be pointed directly at the target (or very close to the target), thus eliminating this beamshape loss.

3.2.4 Search Regimens

Some radar systems have to perform multiple functions nearly simultaneously. This is done by interleaving these functions at a high rate. A prime example is the case in which a radar has to continue to search a volume while also tracking targets that have previously been detected or that represent a threat. Though multifunction radars are becoming more popular, the design for such a system represents a compromise compared with a system that has to perform only a search function or only a track function.

For example, longer wavelengths are favored for search radars, and shorter wavelengths are favored for track functions, as discussed in Chapter 2. As noted earlier, available space and prime power often do not allow for more than one radar for all the required functions. A fixed ground-based air defense system might have the resources to employ multiple radars, but a mobile artillery finding radar may not. The former system may have a source of power from the national power grid, sufficient to operate both a search radar and a tracking radar. The latter system must be small and mobile and must run on a single 60 kVA generator. As another example, a surface ship-based system might have several

radars onboard, but a forward-looking airborne interceptor system has space for only one radar.

With the technology improvements associated with electronically scanned antennas (phased arrays), it is now more efficient to incorporate multiple interleaved functions in a single radar system. Often, search and track functions are combined. There are two distinctly different approaches to interleaving the search and track functions in a single system: *track-while-scan* (TWS) and *search-and-track*.

3.2.4.1 Track-while-Scan

In the TWS mode, the antenna search protocol is established and never modified. When a target is detected as the beam scans in the search volume, a track file is established. The next time the antenna beam passes over this target, a new measurement is made, and its track file is updated. As an example, a 2-D air surveillance radar antenna (as described in Chapter 1) typically has a wide elevation beamwidth to provide coverage at all altitudes but a narrow azimuth beamwidth. The antenna may rotate at 10 revolutions per minute (RPM) as it searches a 360 degree azimuth sector. This means that the beam will be pointed at any given azimuth direction once every 6 seconds, and the track file for a given target will be updated with new measurements at this time interval. Since the beam scan sequence is not changed to accommodate detected targets, this technique does not require the scanning agility of an electronically scanned antenna. As the beam continues to search the volume and more targets are detected, new track files are established for these targets and are updated when the beam scans by them again. In this mode, an arbitrarily large number of targets can be tracked (1,000 or more), limited only by the computer memory and track filter throughput required. The TWS approach is used for air marshalling,[4] air traffic control, and airport surveillance applications, among others. Many of these systems use mechanically scanned antennas.

This approach provides an update rate that is adequate for benign nonthreatening targets such as commercial aircraft, but not for immediately threatening targets such as incoming missiles. An adaptive, more responsive interleaved search-and-track technique for this situation is the search-and-track mode.

3.2.4.2 Search-and-Track

In the search-and-track mode, the radar sequencer (a computer control function often called the *resource manager*) first establishes a search pattern designed to optimize the search function according to the search parameters (e.g., search volume, search frame time, prioritized sectors). If a target is detected in the search volume, then some of the radar resources are devoted to tracking this target. For instance, some percentage of the dwells each second might be assigned to target track updates. Modern search-and-track systems use an antenna beam that is electronically scanned, because the beam must be capable of being moved rapidly between arbitrary positions to optimize the tracking mode. Some legacy airborne interceptor systems used the search-and-track technique with a mechanically scanned antenna, but the time required for repositioning from the search mode to a target track position greatly extended the total search time. As a simple example, consider a radar searching a volume defined as a 90 degree azimuth sector and a 4 degree elevation

[4]The U.S. Navy has a requirement to monitor and control aircraft in the vicinity of an aircraft carrier. This procedure is termed *marshalling*.

sector. When a target is detected, the resource manager allocates whatever resources are required, based on, for example, target size, distance, or speed, for a high-quality track. Assume the resource manager devotes 5% of the dwells to providing measurements to the track algorithm for that target. Thus, 95% of the radar resources are left to continue the search, therefore increasing the search time somewhat. If another target is subsequently detected, another 5% of the resources may be devoted to tracking this second target, leaving 90% of the original radar dwells for searching and further increasing the search time. If 10 targets are being tracked, each using 5% of the radar resources, only 50% of the resources are left to continue the search. In this case, the search frame time will double compared with the original frame time.

This example makes it clear that in the search-and-track protocol, there is a limit to the number of targets that can be tracked simultaneously before there remain too few of the radar resources to continue an effective search. If the search frame time becomes too long, then targets of interest may get through the angular positions being searched between scans. Algorithms are developed in the system software to manage the radar resources to strike an appropriate balance between the search frame time and the number of target tracks maintained.

Some systems combine both search-and-track and track-while-scan functions. The rationale for this is as follows. The frequent updates and agility of a search-and-track system are required to accurately track targets that represent short-term threats and may have high dynamics (velocities and accelerations). Examples of such targets include incoming threats such as anti-ship missiles, fast and low radar cross section (RCS) targets, low altitude cruise missiles, and enemy artillery such as mortars and rockets. Radar systems designed to detect and track such targets are able to detect low RCS targets at long range in the presence of high RCS clutter. They also typically perform target identification functions by analyzing the target amplitude and Doppler characteristics. Such a system is likely to be a medium PRF pulse-Doppler radar and is therefore subject to the range ambiguities. That is, a long-distance low RCS target may be competing with close-in high RCS clutter.

If a target is detected and *confirmed* or *qualified* to be a true target (as opposed to a false alarm), then the target identification process is initiated. If the target is determined to be a threat rather than benign, a track file is initiated. This track initiation process consumes time for each target detected. Due to the detection range of these radar systems, target detections can occur not only for potential threat targets but also for nonthreatening targets such as friendly ground-moving vehicles and helicopters and also for birds, insects, and even turbulent air. Insects and turbulent air will be detected only at short range; however, for a range-ambiguous medium PRF system, a small target that is apparently at close range may be misinterpreted as a true threat target at a longer range. The topic of second-time-around targets, or range ambiguities, is introduced in Chapter 1 and further expanded in Chapters 12 and 17. Chapter 17 describes a technique using multiple CPIs with staggered PRFs within a given antenna dwell to resolve the range and Doppler ambiguities.

There may be many such detections in a single search scan, consuming a large fraction of the radar timeline in the target qualification process. For example, if it takes 100 msec to qualify a target and there are 100 potential target detections in a scan, then the radar will consume the next 10 seconds qualifying targets. Once the "uninteresting" targets are identified, they must still be continually tracked, or else they will be detected again on subsequent scans and have to be qualified repeatedly. However, a high-precision track is not required for these "nuisance" targets. Consequently, a track-while-scan mode can be used to maintain tracks on these targets without consuming large amounts of radar resources.

3.3 OVERVIEW OF DETECTION FUNDAMENTALS

3.3.1 Overview of the Threshold Detection Concept

The concept of *detection* of a target involves deciding, for each azimuth/elevation beam position, whether a target of interest exists in antenna beam. The technique may be as simple as an operator looking at a display and deciding if a given area of the display is "bright" enough relative to the surrounding background to be a target of interest. In most modern radar systems, detection is performed automatically in the signal/data processor. It is accomplished by establishing a threshold signal level (voltage) on the basis of the current interference (e.g., external noise, clutter, internal receiver thermal noise) voltage and then by deciding on the presence of a target by comparing the signal level in every cell with that threshold. If the signal level exceeds the threshold, then the presence of a target is declared. If the signal does not exceed the threshold, then no target is declared. This concept is shown in Figure 3-2. The detection in bin #50 may in fact be from a target, or it may be a large noise spike, creating a *false alarm*.

The detection process is performed on the received signal after whatever processing the signal experiences. It may be that a decision is made on the basis of a single transmitted pulse, though this is rare. More often, several pulses are transmitted, and the resulting received signal is integrated or processed in some way to improve the SNR compared with the single-pulse case. In any case, to detect the target signal with some reasonable probability and to reject noise, the signal must be larger than the noise. Later in this chapter the relationship between SNR and P_D will be explored.

If the interference is known to consist only of thermal noise in the receiver, then the receiver gains can be set such that the noise voltage will be at a known level. The detection threshold can then be set at a fixed voltage, far enough above that noise level to keep the probability of a false alarm (threshold crossing due to noise alone) at an acceptably low level. However, the interference is seldom this well known. In many radars the interference consists not only of receiver noise but also of clutter and noise jamming. The interference due to jamming and clutter will be quite variable as a function of range, angle, and Doppler cells in the vicinity of a target. Consequently, the interference level can vary by many dB during operation so that a fixed threshold level is not feasible. Particularly in modern radars, the threshold is often adaptive, automatically adjusting to the local interference level to

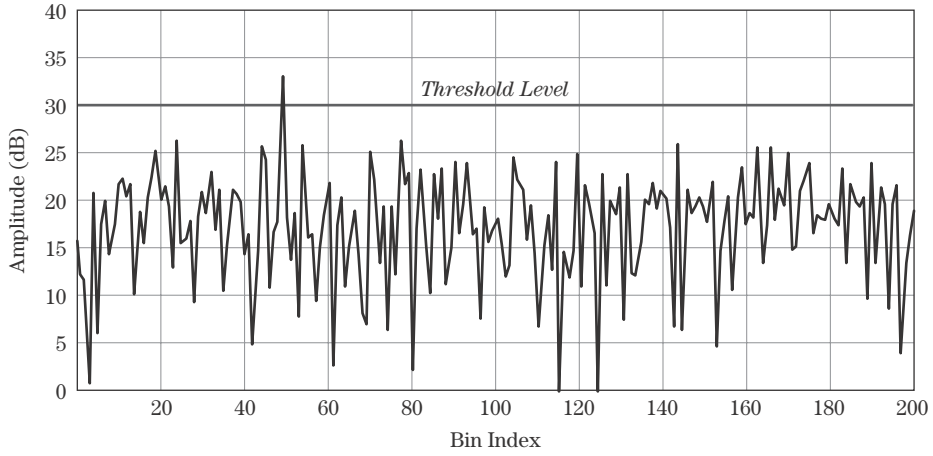

FIGURE 3-2 Concept of threshold detection. In this example, a target would be declared at bin #50.

result in a constant false alarm rate (CFAR). The target signal, when present, must exceed the threshold to be detected. Details of CFAR processing are described in Chapter 16.

The description so far is of detection on the basis of amplitude alone; the amplitude of the target signal must exceed the threshold voltage determined by the interfering signal by a sufficient amount. A more severe case exists when the dominant source is clutter and especially if its amplitude exceeds that of the target signal. In this case, spectral signal processing is often employed (moving target indication [MTI] or pulse-Doppler processing) to reduce the clutter level below that of the target signal. In cases where the dominant interference is jamming and its level exceeds that of the target, often angle-of-arrival processing (e.g., sidelobe cancellation, adaptive beamforming) may be used. Systems suffering significant clutter and jamming interference may use a combination of both, called space-time adaptive processing (STAP). The detection process is performed on the output of such processors. General signal processing techniques are described in Chapter 14, and Doppler processing is described in Chapter 17.

The radar user is usually most interested in knowing (or specifying) the probability of detecting a given target, P_D, and the probability of a false alarm, P_{FA}, caused by noise. This chapter introduces the process for developing the relationship among P_D, P_{FA}, and SNR. Curves describing these relationships are often called *receiver operating curves* or *receiver operating characteristics* (ROCs).

The intent of the remainder of this chapter is to build an understanding of the issues associated with detecting a desired target in the presence of unavoidable interfering signals. The primary emphasis will be on the simplest case of a nonfluctuating target signal and noise-like (i.e., Rayleigh-distributed) interference, though some extensions will be mentioned. Chapter 15 extends the topic of detection to include the effects of the Swerling fluctuating target models, and Chapter 16 describes the implementation and performance of systems that use CFAR techniques to set the threshold level adaptively.

3.3.2 Probabilities of False Alarm and Detection

The noise at the receiver output is a randomly varying voltage. Because of the effect of multiple scatterers constructively and destructively interfering with each other, most targets of interest also present echo voltages that vary randomly from pulse to pulse, from dwell to dwell, or from scan to scan, as described in Chapters 6 and 7. However, even if the target is modeled as a constant echo voltage, the output voltage of the receiver when a target is present is the complex (amplitude and phase) combination of the target echo and noise, so it still varies randomly. Therefore, the process of detecting the presence of a target on the basis of the signal voltage is a statistical process, with a probability of detection, P_D, usually less than unity, and some probability of false alarm, P_{FA}, usually greater than zero.

The fluctuating noise and target-plus-noise voltages, v, are characterized in terms of their probability density functions (PDFs), $p_v(v)$, which are functions describing the relative likelihood that a random variable will take on various values. For example, the Gaussian or normal PDF in Figure 3-3 shows that the voltage, v, can take on positive and negative values with equal likelihood, can range from large negative to large positive values, but is more likely to take on values near zero than larger values. The likelihood of taking on values outside of the range of about -2 to $+2$ is quite small in this example.

Probability density functions are used to compute probabilities. For example, the probability that the random variable, v, exceeds some threshold voltage, V_t (a hypothetical

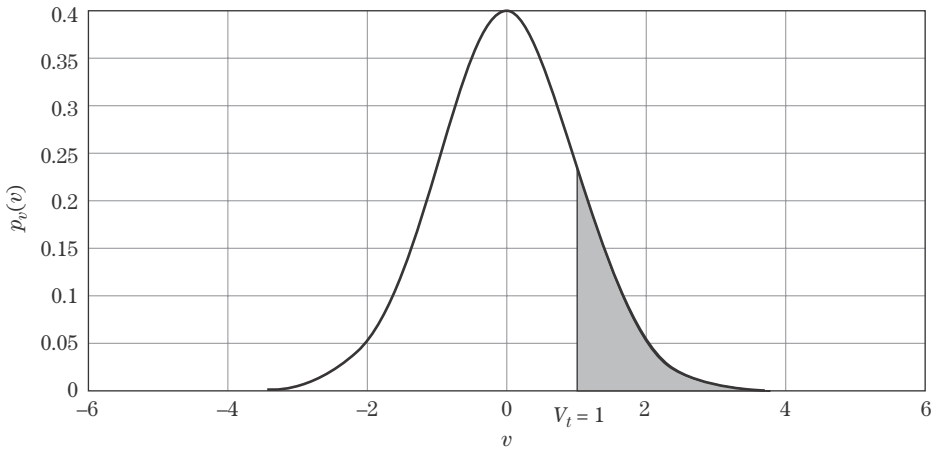

FIGURE 3-3 ■ Gaussian PDF for a voltage, v.

value of 1 for V_t is indicated in Figure 3-3), is the area under the PDF in the region where $v > V_t$, which is

$$\text{Probability}\{v > V_t\} = \int_{V_t}^{\infty} p_v(v)\, dv \tag{3.7}$$

To apply this equation to determine the P_{FA} for a given threshold voltage, suppose the PDF of the noise voltage is denoted as $p_i(v)$. A voltage threshold, V_t, is established at some level sufficiently above the mean value of the noise voltage to limit false alarms to an acceptable rate. The false alarm probability, P_{FA}, is the integral of the noise probability density function from the threshold voltage to positive infinity:

$$P_{FA} = \int_{Vt}^{\infty} p_i(v)\, dv \tag{3.8}$$

By increasing or decreasing the threshold level, V_t, P_{FA} can be decreased or increased. Thus, P_{FA} can be set at any desired level by proper choice of V_t. Determining the required threshold voltage requires solving (3.8) for V_t, given the desired P_{FA}. This process will be described in Section 3.3.3.

Once the threshold is established on the basis of the noise PDF and desired P_{FA}, the probability of detecting a target depends on the PDF of the signal-plus-noise voltage, p_{s+i}, which depends on the fluctuation statistics of both the noise and the target signals as well as on the SNR. The target detection probability, P_D, is the integral of the signal-plus-noise PDF from the threshold voltage to positive infinity:

$$P_D = \int_{Vt}^{\infty} p_{s+i}(v)\, dv \tag{3.9}$$

3.3.3 Noise PDF and False Alarms

As described already, in the absence of any target signal there is an opportunity for an interfering noise voltage to be interpreted as a target signal. A false detection of such

a noise signal, caused by the noise voltage exceeding the voltage threshold, is called a false alarm. The fraction of the detection tests in which a false alarm occurs is called the probability of false alarm, P_{FA}. To analytically determine the probability of false alarm for a given noise amplitude and threshold voltage, the PDF of the noise must be known. This requires an understanding of the noise statistics and detector design.

Whereas noncoherent radar systems detect only the amplitude of the received signal, most modern radar systems are coherent and process the received signal as a vector with amplitude, v, and signal phase, ϕ. The most common detector circuit is a synchronous detector that develops the *in-phase* (I) component of the vector and the *quadrature* (Q) phase component. Even in more modern systems in which the signal is sampled at the intermediate frequency (IF) with a single analog-to-digital converter (ADC), an algorithm implemented in the system firmware constructs the I and Q components of the signal for processing. A description of the direct sampling approach is given in Chapter 11.

When the interfering signal is thermal noise, each of these signals is a normally distributed random voltage with zero mean [2]. The signal amplitude, v, is found as

$$v = \sqrt{I^2 + Q^2} \tag{3.10}$$

Equation (3.10) is referred to as a *linear detector*, and the amplitude signal, r, is often called the radar *video* signal. It can be shown that when the I and Q signals are zero mean Gaussian (i.e., normal) voltages as previously described, the resulting noise amplitude is distributed according to the Rayleigh PDF [1]. In some systems the square root function is left out of equation (3.10), resulting in a *square-law* detector. In some legacy systems, mostly noncoherent ground mapping radars, the detected signal amplitude is processed by a logarithmic amplifier. In this case the detector is called a *log detector,* and the output is sometimes called log-video. Log detectors were used to compress the wide dynamic range of the received signals to match the limited dynamic range of the display. Neither log nor square law detectors are as popular as the linear detector in modern radar systems. For this reason, the following analysis will be directed toward linear detection.

The Rayleigh PDF is

$$p_i(v) = \frac{v}{\sigma_n^2} \exp\left(\frac{-v^2}{2\sigma_n^2}\right) \tag{3.11}$$

where v is the detected envelope voltage and σ_n^2 is the mean square voltage or variance of the noise, which is simply the average noise power at the detector output. Figure 3-4 is a plot of the Rayleigh PDF when the noise power $\sigma_n^2 = 0.04$, with an arbitrary but reasonable location for a threshold voltage, V_t, indicated at $v = 0.64$. By inspection, the particular threshold voltage shown would result in a reasonably low P_{FA}; that is, it appears that a small percentage of the area under the curve is to the right of the threshold. It should be understood that, for most systems, false alarms do occur. Seldom is a threshold established that is so far above the mean noise level that no interfering signal ever exceeds the threshold.

Normally, the probability of a false alarm is low. It is typically further reduced by requiring that a target detection must occur twice: once in the initial search and subsequently in a *confirmation* or *verification* process. If there is an initial detection in the search mode, then the system is directed to immediately "look" for the target at the same range/angle/Doppler cell. If the subsequent detection is made, the detection is deemed to be a target. If not, the original detection is deemed to be a false alarm. This process greatly

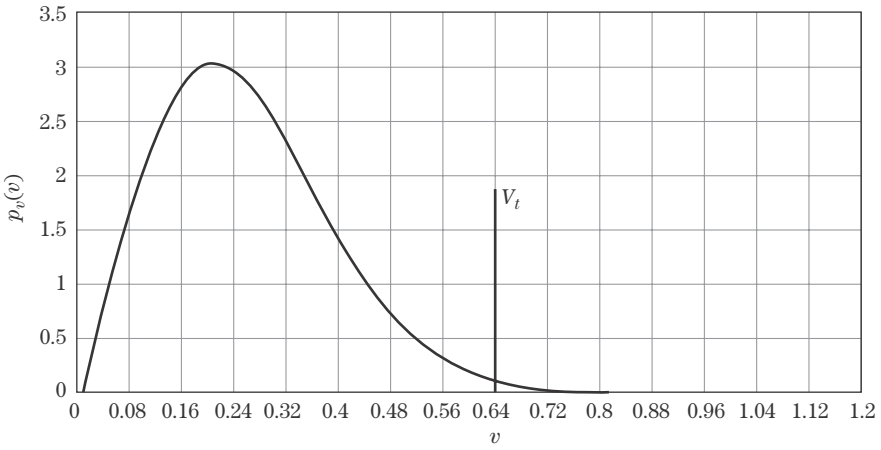

FIGURE 3-4 ■ Rayleigh distribution with an arbitrary threshold.

reduces the probability that a noise spike will initiate a track event. As an example, the system may be designed to produce, on average, one false alarm per complete antenna scan pattern.

For a single sample of Rayleigh-distributed noise, the probability of false alarm is found from equations (3.8) and (3.11):

$$P_{FA} = \int_{V_T}^{\infty} \frac{r}{\sigma_n^2} e^{-r^2/2\sigma_n^2} dr = e^{-V_T^2/2\sigma_n^2} \tag{3.12}$$

Solving for V_T provides the threshold voltage required to obtain a desired P_{FA}:

$$V_T = \sqrt{2\sigma_n^2 \ln(1/P_{FA})} \tag{3.13}$$

Thus, given knowledge of the desired P_{FA}, noise statistics, and detector design, it is possible to determine the threshold level that should be used at the detector output. Note that the target signal statistics are not involved in setting the threshold level.

As mentioned previously, search systems are designed such that if a detection is made at a given position for a given dwell, understanding that such detection may be a false alarm, a subsequent confirmation dwell at the same position is processed to see if the receiver output still exceeds the threshold. For a false alarm, the likelihood of a subsequent false detection is remote, usually settling the question of whether the detection was a false alarm or a true target. However, even this process is not perfect since there is still a small likelihood that the false alarm will persist or that a true target will not. Assume that the probability of a false alarm is independent on each of n dwells. The probability of observing a false alarm on all n dwells, $P_{FA}(n)$, is related to the single-dwell probability of false alarm, $P_{FA}(1)$, by

$$P_{FA}(n) = [P_{FA}(1)]^n \tag{3.14}$$

The likelihood that a false alarm will occur for two consecutive trials is P_{FA}^2, for three trials is P_{FA}^3, and so forth. As an example, for a single-trial P_{FA} of 10^{-4}, the two-trial P_{FA} is 10^{-8}.

Consider how the use of confirmation dwells affects the false alarm rate and search time for a hypothetical search radar. Continuing the example given earlier, suppose the radar has 90 beam positions for a given search sector, 333 range bins for each beam

position, and 32 Doppler bins for each range/azimuth position. There will then be 959,040 opportunities for a false alarm in a complete search scan. For a single-dwell false alarm probability of 10^{-5}, there will be about 9.6 false alarms during the scan on average. The user normally has to determine the acceptable false alarm rate for the system, one that does not overload the signal processor or fill the display with false alarms, making it difficult to sort out the actual target detections. The use of a confirmation dwell after each regular dwell could reduce the overall P_{FA} to $(10^{-5})^2 = 10^{-10}$ so that there would be a false alarm after confirmation in only 1 in 10,000 scans, on average. Continuing with the search example given in Section 3.2.2, if each confirmation dwell (T_d or *CPI*), requires 2 ms, the same as the regular dwells, then 9.6 confirmation processes will add 19.2 ms to each nominally 900 ms search time. This is likely an acceptable expense, the alternative being to use a higher threshold voltage, which would reduce the probability of detection. However, if too many confirmation dwells are initiated, the radar search time would suffer significantly. For instance, if the P_{FA} were 10^{-4}, then there would be about 96 false alarms per scan on average. The confirmation dwells would then add about 192 msec to every 900 ms dwell, a 21.3% increase in search time. This increase would probably be considered an inefficient use of time.

3.3.4 Signal-Plus-Noise PDF: Target Detection

If, at some point during the search, the radar antenna is pointed in the direction of a target, then at the appropriate range there will be a signal resulting from the target. Of course, the noise signal is still present, so the signal in the target cell is a complex combination of target signal and the noise. This signal is the one the radar is intended to detect. Since it is composed of a combination of two signals—one a varying noise signal and the other a target signal—then there will be a variation to the combined signal. Therefore, it has a PDF that is dependent on the target signal fluctuation properties as well as the interfering signal properties. Target fluctuations are characterized in Chapter 7, and their effect on detection is described in Chapter 15. Only the simpler case of a nonfluctuating target echo is considered here to illustrate detection concepts.

For a nonfluctuating target, the PDF of the target-plus-noise signal voltage was originally shown by Rice [2] and was later discussed in [3,4] to be of the *Rician* form. This PDF is defined in equation (3.15) and plotted in Figure 3-5 along with the noise-only Rayleigh PDF for comparison.

$$p_{s+i}(v) = \frac{v}{\sigma_n^2} \exp\left[-\left(v^2 + v_{s+i}^2\right)/2\sigma_n^2\right] I_0\left(v v_{s+i}/\sigma_n^2\right) \tag{3.15}$$

where v_{s+i} is the detected signal voltage, and $I_0(\cdot)$ is the modified Bessel function of the first kind and zero order.

The procedure for determining the probability of detection given the target-plus-noise PDF is the same as for determining P_{FA} given the noise-only PDF. Using the threshold determined from the noise statistics in equation (3.13), the PDF is integrated from the threshold voltage to positive infinity:

$$P_D = \int_{V_t}^{\infty} p_{s+i}(v)dv = \int_{V_t}^{\infty} \frac{v}{\sigma_n^2} \exp\left[-\left(v^2 + v_{s+i}^2\right)/2\sigma_n^2\right] I_0\left(v v_{s+i}/\sigma_n^2\right)dv \tag{3.16}$$

This integral has no easy closed-form solution. Rather, it is defined as a new special function called *Marcum's Q function,* Q_M, discussed further in Chapter 15 and [3,5].

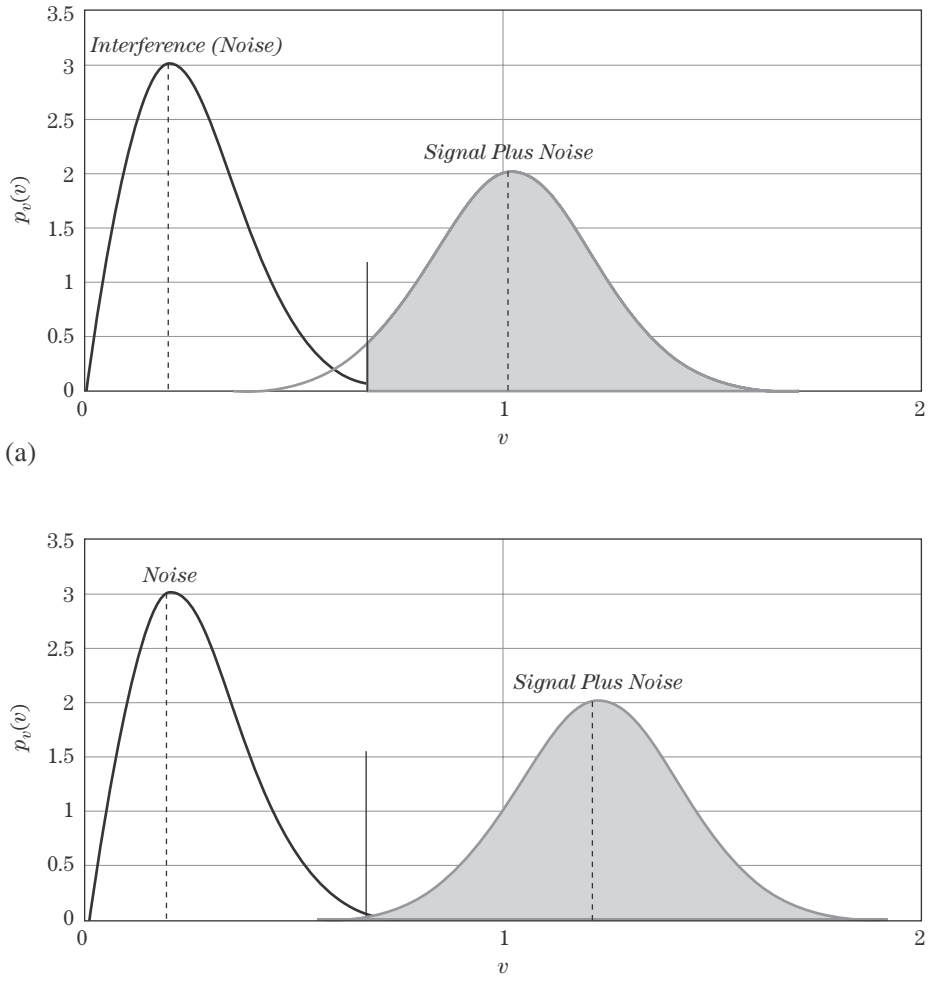

FIGURE 3-5 ■ (a) Noise-like distribution, with target-plus-noise distribution. (b) Noise-like distribution, with target-plus-noise distribution, demonstrating the higher P_D achieved with a higher SNR.

Routines to compute Marcum's Q function are available in MATLAB and similar computational systems. In addition, various analytic approximations for the calculation of ROCs for the case of a nonfluctuating target in noise are discussed in Section 3.3.7 of this chapter.

For the case shown in Figure 3-5a, P_D will clearly be significantly greater than the P_{FA}; that is, a relatively high percentage of the area under the signal-plus-noise curve is above the threshold. This figure also again makes clear that, as the threshold is raised or lowered, both P_D and P_{FA} will be decreased (higher threshold) or increased (lower threshold).

Moving the threshold to the left (lower) or right (higher) changes the P_D and P_{FA} together for a given SNR. To get a higher P_D without increasing the P_{FA} requires that the two curves be separated more—a higher SNR is required. Figure 3-5b demonstrates that increasing the SNR while maintaining the same threshold setting (constant P_{FA}) increases the P_D. Conversely, if the SNR were to be reduced, then the curves would overlap more, and a lower P_D would result for a given threshold. This suggests that a curve of P_{FA} versus P_D for given SNR or of P_D versus SNR for a given P_{FA} would be valuable. Such curves are the topic of the next section.

By definition, the total area under a PDF curve is always unity, so P_{FA} and P_D will be less than or equal to 1. If the target signal is larger than the noise signal by a great enough margin (SNR $\gg$ 0 dB), then the threshold can be set so that P_{FA} will be nearly zero yet P_D will be nearly unity. Required values of P_D and P_{FA} are determined from higher-level system requirements and can vary greatly. However, typically P_D is specified to be in the neighborhood of 50% to 90% for a P_{FA} on the order of 10^{-4} to 10^{-6}. Clearly, if the interfering signal is of higher amplitude than the target signal (SNR $<$ 0 dB), then an unacceptably low P_D and high P_{FA} will result. This condition would suggest using some signal processing technique to reduce or cancel the noise or enhance the target signal, increasing the SNR in either case.

If the P_D and P_{FA} performance is not as good as required—that is, if the P_{FA} is too high for a required P_D or the P_D is too low for a required P_{FA}—then something must be done to better separate the noise and target-plus-noise PDFs on the plot. Either the noise has to be moved to the left (reduced in amplitude), or the target has to be moved to the right (increased in amplitude). Alternatively, the variance of the noise can be reduced, which will narrow both PDFs. These effects can be obtained only by modifying the system in some way to increase the SNR, either by changing the hardware or applying additional signal processing to adjust one of more of the terms in the RRE described in the Chapter 2. For example, the designer could increase the transmit power, the dwell time, or the antenna size (and thus gain).

3.3.5 Receiver Operating Curves

The previously shown plots depict the PDFs for noise and target-plus-noise, with an arbitrary threshold voltage plotted. The calculations already described will produce the P_D and P_{FA} for a given threshold and SNR. If the threshold is varied, a series of combinations of P_D and P_{FA} result that describe the trade-off between detection and false alarm probabilities for a given SNR. A succinct way to capture these trade-offs for a large number of radar system operating conditions is to plot one variable versus another variable for different fixed values of the third variable. The ROC is just such a curve. An example of an ROC is shown in Figure 3-6, which presents a set of curves of the SNR required to achieve a given P_D, with P_{FA} as a parameter, for a nonfluctuating target. Two alternative formats for the ROC curves are found in the literature. Some authors present plots of P_D versus SNR with

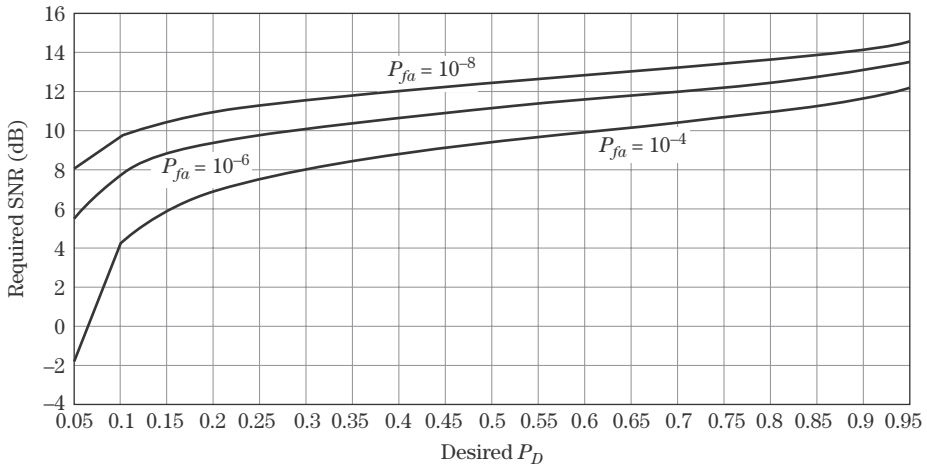

FIGURE 3-6 ■ SNR required to achieve a given P_D, for several P_{FA}'s, for a nonfluctuating (SW0) target in noise.

P_{FA} as a parameter, while others present plots of P_D versus P_{FA} with SNR as a parameter. A number of texts [e.g., 7–10] present ROC curves for a variety of conditions, most often for the case of nonfluctuating and fluctuating target signals in white noise. Results for other target fluctuation and interference-other-than-noise models are available in the literature. These results are derived using the same general strategies already described but differ in the details of the PDFs involved and thus the results obtained. Chapter 7 discusses target reflectivity statistical modeling, and Chapter 15 discusses detection performance for various target fluctuation models.

3.3.6 Fluctuating Targets

In addition to the fact that the noise signal fluctuates, it is also true that the target signal fluctuates for most real targets. Peter Swerling developed a set of four statistical models that describe four different target fluctuation conditions [8]. The four cases include two PDF models (Rayleigh and 4-th degree chi-square) and two fluctuation rates (dwell to dwell[5] and pulse to pulse.) They are labeled Swerling 1, 2, 3, and 4 (SW1, SW2, SW3, and SW4, respectively). Table 3-1 shows the PDFs and fluctuation characteristics for the four models. A nonfluctuating target is sometimes called a Swerling 0 (SW0) or a Marcum target model. These as well as other target models are discussed in detail in Chapter 7.

Table 3-2 gives some previously calculated commonly specified P_{FA} and P_D values and the required SNR in dB for the five common target models. These points were extracted from plots in [10]. For a nonfluctuating target in noise, reliable detection (90% P_D) is achieved with a reasonable (10^{-6}) P_{FA} given an SNR of about 13.2 dB. In the case of a fluctuating target signal, the PDF of the target-plus-noise is wider, leading to a lower P_D than for a nonfluctuating target at the same SNR. Thus, a higher SNR is required to achieve 90% P_D. In fact, an SNR of 17.1 to 21 dB is required for to achieve $P_D = 90\%$ at $P_{FA} = 10^{-6}$ versus 13.2 dB for the nonfluctuating case. Lower SNR values provide

TABLE 3-1 ■ Swerling Models

	Fluctuation Period	
Probability Density Function of RCS	Dwell-to-Dwell	Pulse-to-Pulse
Rayleigh	Case 1	Case 2
Chi-square, degree 4	Case 3	Case 4

TABLE 3-2 ■ Required SNR for Various Target Fluctuation Models

	P_D	SW0	SW1	SW2	SW3	SW4
$P_{FA} = 10^{-4}$	50	9.2	10.8	10.5	11	9.8
	90	11.6	19.2	19	16.5	15.2
$P_{FA} = 10^{-6}$	50	11.1	12.8	12.5	11.8	11.8
	90	13.2	21	21	17.2	17.1

[5]Classically, the slowly fluctuating target was described as fluctuating from scan to scan; however, with modern system signal processing, the term *dwell to dwell* is often used.

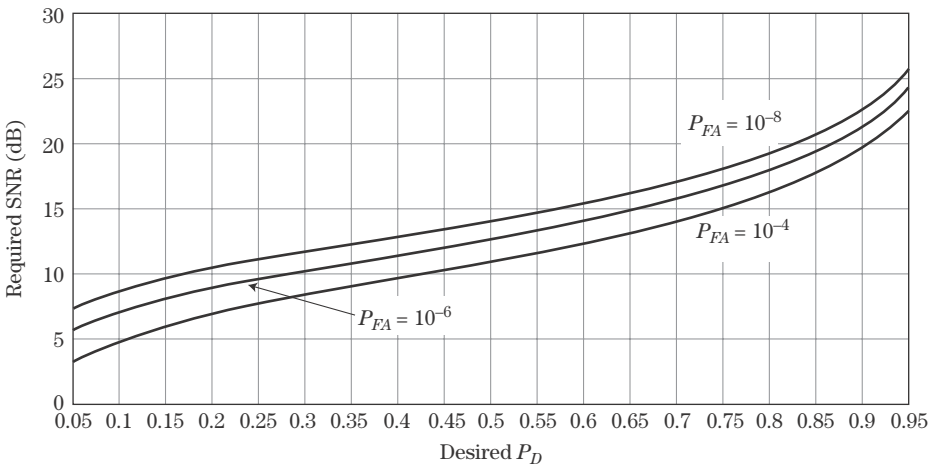

FIGURE 3-7 ■ SNR required to achieve a given P_D, for several values of P_{FA}, for fluctuating (SW1) target in noise.

lower detection probabilities, which may still be acceptable if detection can be made on the basis of several opportunities, such as over several antenna scans or several consecutive dwell periods. The system designer thus can trade radar sensitivity versus observation time in the overall system design. Figure 3-7 is an example of the ROC curves for the Swerling 1 case. This can be compared with Figure 3-6, which present the same data for the nonfluctuating target case. Chapter 7 describes the statistical nature of most target signals, showing that most targets of interest are usually fluctuating rather than of fixed amplitude. Details of the calculation of P_D and P_{FA} and corresponding ROC curves for the fluctuating target cases are given there.

Because the PDF of a fluctuating target has a higher variance (i.e., is "spread" more) than that of a nonfluctuating target, for a given SNR the target and noise PDF curves will overlap more. Therefore, for a given threshold setting, the P_D will be lower for the fluctuating target. Figure 3-8 compares the data of Figures 3-6 and 3-7 to show the SNR as a function of P_D for an SW0 (nonfluctuating) target and an SW1 target. Notice that for levels of P_D, from 50% to 95%, the SNR required for a fluctuating target RCS is significantly higher than that for a nonfluctuating target.

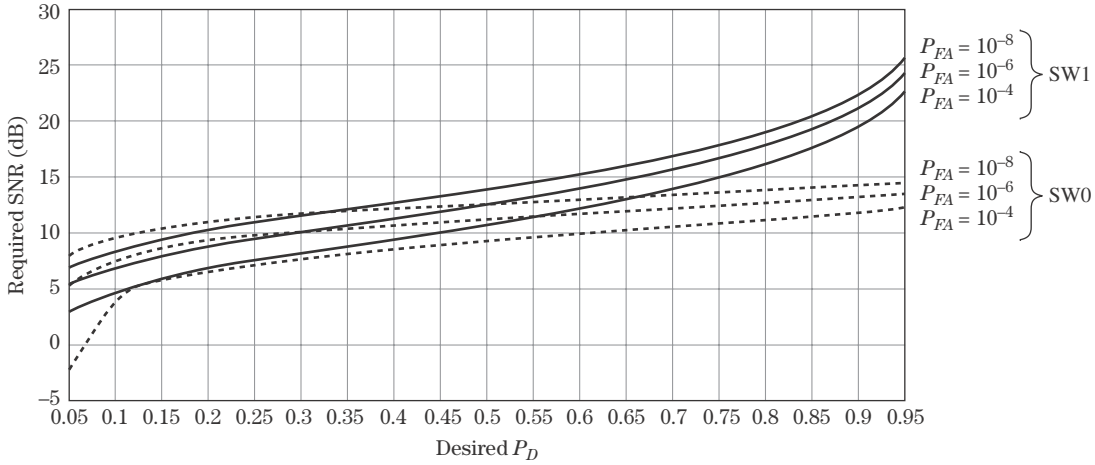

FIGURE 3-8 ■ SNR required to achieve a given P_D, several values of P_{FA}, for nonfluctuating (SW0) and fluctuating (SW1) target models.

3.3.7 Interference Other than Noise

The curves that have been plotted and presented in many standard radar texts give the P_D and P_{FA} for various values of SNR, where the interfering signal is Rayleigh-distributed after the linear detector. Thermal receiver noise in the radar and noise jamming usually satisfy this condition. Clutter interference, on the other hand, usually does not. The PDFs for clutter are proposed in many radar texts and journal articles. Some common models are Weibull, log-normal, and K-distributed [11–13]. Chapter 6 provides a summary of the clutter statistics normally encountered in modern radars.

It is not the intent of this chapter to fully describe these models; however, it is the intent to build an appreciation for the effects of these fluctuation models on target detection statistics. In general, the nature of the PDFs for distributions associated with clutter is such that they have longer "tails" in the PDFs. The effect is to increase the P_{FA} for a given threshold setting. That is, for a given mean value, there is a higher probability that the signal reaches higher amplitudes than that of noise so, compared with noise, more of the area under the curve is to the right of a given threshold. If a given P_{FA} is to be maintained if the clutter signal increases, the threshold must be increased to maintain the P_{FA} at the desired value. Doing so will lower the P_D for a given signal-to-interference ratio because less of the area under the target curve will be to the right of the higher threshold. In Figure 3-9, a hypothetical but typical clutter PDF (Weibull) is plotted in addition to the Rayleigh distribution to demonstrate the effect of the longer tail in the clutter distribution. The clutter distribution will produce a higher P_{FA} for the threshold setting shown. Therefore, the threshold will have to increase (move to the right) to recover the desired P_{FA}. As depicted in the figure, if the same false alarm probability is desired due to Weibull-distributed clutter as for Rayleigh-distributed noise, the threshold must increase, lowering the P_D for a given signal voltage. In fact, depending on the particular clutter encountered, the effect of these extended tails can be severe. In some cases, to maintain a given P_{FA} and P_D, the signal-to-clutter ratio must be 10 or even 20 dB higher than if the interference is noise-like. It is in these conditions that some method for reducing the clutter signal must be employed. Moving target indication and pulse Doppler processing techniques are the most common of these. These techniques, which are discussed in Chapter 17, reduce the clutter signal significantly.

The clutter signal is often significantly larger in amplitude than the target signal. This is because a clutter cell illuminated by the radar can result in a very large clutter area

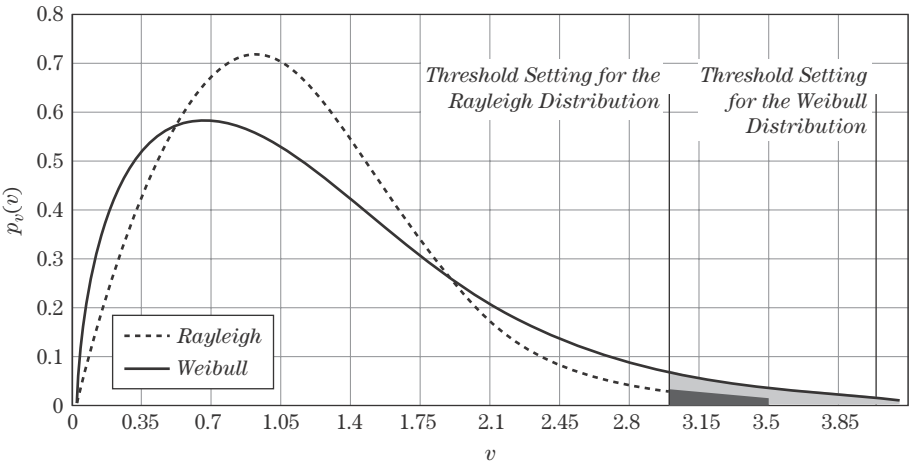

FIGURE 3-9 ■ Example clutter PDF compared with noise.

which, when multiplied by the average reflectivity of the clutter in the cell, produces a large effective RCS. The target may be quite small and, for stealth targets, smaller yet. In this case, the target signal must be separated from the clutter signal in the spectral domain, usually employing pulse-Doppler FFT processing. Since it is impractical to completely confine the clutter signal to only a few Doppler bins, there will still be some residual clutter signal persisting in the vicinity of the target signal. Thus, the question is what is the shape of the residual clutter distribution curve after the processing? The central limit theorem would suggest that since 20 or 30 samples are integrated, the new distribution might be Gaussian. This requires that the individual interference samples are statistically independent. Are the samples independent? This depends on the PRF, the decorrelation time of the clutter, and the dwell time. For most cases, the samples are not independent, suggesting that the residual clutter signal after the processor is the same shape as the original distribution (e.g., Weibull).

3.3.8 Some Closed-Form Solutions

Exact calculation of the probability of detection requires solving the integral in equation (3.16) or, equivalently, evaluation of the Marcum's Q function. While this is relatively easy using modern analysis tools such as MATLAB, it is valuable to have a simple, closed-form solution for the mathematical procedures previously described that can be solved using a spreadsheet or even a calculator. Fortunately, excellent approximations using simple formulae are available. These approximations are applicable for estimates of SNR with precision on the order of 0.5 dB and if extreme values of P_D and P_{FA} are not desired. In this chapter, Albersheim's approximation for the detection performance in the nonfluctuating target RCS case is presented. Also given are the exact results for a Swerling 1 target model when only a single sample is used for detection. The cases summarized here provide examples of detection performance and demonstrate the advantage of multiple-dwell detection techniques.

3.3.8.1 Approximate Detection Results for a Nonfluctuating Target

Albersheim's equation [14,15] is an empirically derived equation relating P_D, P_{FA}, the number of pulses noncoherently integrated, N, and the single-pulse SNR. It applies to Swerling 0 (nonfluctuating) targets and a linear detector, though it also provides good

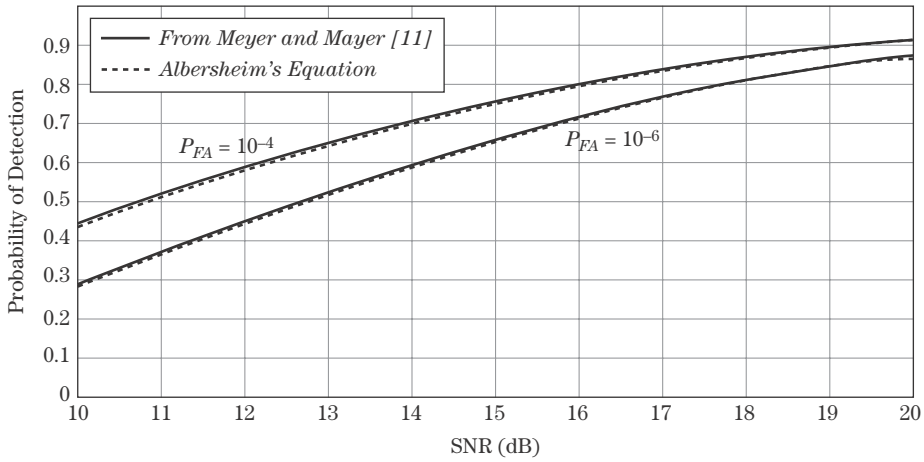

FIGURE 3-10 ■ SNR versus P_D for a Swerling 0 target using Albersheim's equation, plotted with tabulated results from Mayer and Meyer [10].

estimates for a square law detector. This is a very good approximation for values of P_D between 0.1 and 0.9 and of P_{FA} between 10^{-7} and 10^{-3}. Figure 3-10 shows ROCs computed using Albersheim's equation for P_{FA} values of 10^{-4} and 10^{-6}. The figure also shows the exact results from [10]. Note the excellent agreement between the approximated and exact results for these cases.

Albersheim's estimate of the required SNR (in dB) to achieve a given P_D and P_{FA} when N independent samples are noncoherently integrated is

$$SNR\ (\text{dB}) = -5\log_{10} N + \left(6.2 + \frac{4.54}{\sqrt{N + 0.44}}\right)\log_{10}(A + 0.12AB + 1.7B) \quad (3.17)$$

where

$$A = \ln(0.62/P_{FA}) \quad (3.18)$$

and

$$B = \ln\left(\frac{P_D}{1 - P_D}\right) \quad (3.19)$$

It is also possible to rearrange Albersheim's equation to solve for P_D given P_{FA}, N, and the single-pulse SNR. Details are given in Chapter 15 and [17].

Though Albersheim's equation provides simple, closed-form method for calculation, it applies only to a nonfluctuating target, which is seldom a good model in practice. In Chapter 15, an approximation similar in spirit to Albersheim's equation, but applicable to all of the Swerling models, is presented [16].

3.3.8.2 Swerling 1 Target Model

The Swerling models for describing the statistics of target fluctuations were described in Section 3.3.6. For the purpose of providing an example of an ROC for fluctuating targets, a Swerling 1 target model with a single-echo sample (no noncoherent integration of multiple samples) will be considered here. Chapter 7 presents the analysis showing that a Swerling 1 target is appropriate for targets composed of multiple scatterers of roughly the same RCS. The resulting voltage PDF for this target is a Rayleigh distribution. In fact, this is the same distribution used to describe receiver noise. When combined with the Rayleigh noise distribution, the target-plus-noise PDF is still a Rayleigh distribution [19]. Specifically, the target-plus-noise PDF is of the form

$$p_{s+i}(v) = \frac{v}{S + \sigma_n^2}\exp\left(\frac{-v^2}{2(S + \sigma_n^2)}\right) \quad (3.20)$$

where S is the mean target echo power, and σ_n^2 is the mean noise power. The probability of detection integral is

$$P_D = \int_{V_t}^{\infty} p_{s+i}(v)\,dv = \int_{V_t}^{\infty} \frac{v}{S + \sigma_n^2}\exp\left[-\frac{v^2}{2(S + \sigma_n^2)}\right]dv \quad (3.21)$$

Computing this integral gives the probability of detection as

$$P_D = \exp\left[\frac{-V_t}{1 + SNR}\right] \quad (3.22)$$

where $SNR = S/\sigma_n^2$. In (3.22), V_t and SNR are linear (not dB) values. Using (3.13) it can be shown that the relationship between P_D and P_{FA} for this case is the simple relationship

$$P_D = (P_{FA})^{1/(1+SNR)} \tag{3.23}$$

Equation (3.23) applies only to the case of a Swerling 1 target in white noise, with detection based on only a single sample. This "single sample" may be developed by coherently integrating multiple pulses or the results of multiple CPIs. However, it can not include any noncoherent integration.

3.3.9 Multiple-Dwell Detection Principles: Cumulative P_D

To determine the dwell time required at each beam position, it is necessary to determine the signal-to-noise ratio required to achieve the desired P_D and P_{FA} for a target at maximum range. As an example, for a P_D of 90%, a P_{FA} of 10^{-6}, and a Swerling 2 target, the SNR required is 21 dB. Given the available average power, antenna gain, wavelength, minimum target RCS, receiver noise figure, system losses, and maximum range, equation (2.30) can be used to determine the dwell time to achieve the required SNR of 21 dB.

At first, it might seem that a P_D of 90% is not sufficient to detect a threat with adequate certainty. In fact, radar systems often combine the results from multiple opportunities to detect a target, improving the detection probability. The probability of detecting the target at least once in n dwells, $P_D(n)$, is higher than the probability of detection for a single dwell, $P_D(1)$. For example, if the probability of detection on a single dwell is $P_D(1)$, the probability of detecting the target at least once in n tries is

$$P_D(n) = 1 - [1 - P_D(1)]^n \tag{3.24}$$

provided that the detection results on each individual dwell are statistically independent. If $P_D(1) = 90\%$, then the cumulative probability for two tries will be $P_D(2) = 99\%$ and for three tries will be $P_D(3) = 99.9\%$.

The use of multiple dwells to improve detection probability presents an opportunity for a trade-off of radar detection performance for time. For example, if a 99% P_D was required on a *single* dwell for the previous Swerling 2 example, the SNR would have to be about 30 dB, about 9 dB higher than that required for 90% P_D. Using a second dwell with the 90% P_D doubles the time required to detect the target but saves about 9 dB of radar SNR requirements. This translates into some combination of reduced transmit power, reduced antenna gain, or reduced signal processing gain requirements.

Of course, the false alarm probability is also affected by the use of multiple dwells. It is normally not desirable to have P_{FA} increase due to the multiple dwells, as P_D did. The equation for cumulative P_{FA} is the same as equation (3.24), with P_{FA} substituted for P_D. Because the single-dwell false alarm probability is usually a very small number, the result is well approximated by the simpler equation

$$P_{FA}(n) \approx n \cdot P_{FA}(1) \tag{3.25}$$

Thus, for a three-look cumulative $P_{FA}(3)$ of 10^{-6}, $P_{FA}(1)$ for a single dwell would have to be 0.333×10^{-6}. This modest reduction in the allowable single-dwell P_{FA} will increase the required SNR but will be only a small amount compared with the additional SNR required to achieve a P_D of 99.9% in a single look.

3.3.10 *m*-of-*n* Detection Criterion

Instead of detecting a target on the basis of at least one detection in n tries, system designers often require that some number m or more detections be required in n tries before a target detection is accepted. If m and n are properly chosen, this rule has the effect of both significantly reducing the P_{FA} and increasing the P_D compared with the single-dwell case. The probability of a threshold crossing on at least m-of-n tries is found from the binomial theorem [1,18,19]:

$$P(m, n) = \sum_{k=m}^{n} \frac{n!}{k!(n-k)!} P^k (1-P)^{n-k} \tag{3.26}$$

Here, P is the probability of a threshold crossing on a single trial. Equation (3.26) applies both to false alarms as well as detections. If $P = P_{FA}(1)$, then it gives the cumulative false alarm probability for an m-of-n test; if $P = P_D(1)$, then it gives the cumulative detection probability for an m-of-n test. For a commonly used 2 of 3 rule ($m = 2$, $n = 3$), (3.26) reduces to

$$P(2, 3) = 3P^2 - 2P^3 \tag{3.27}$$

and for 2 of 4 it becomes

$$P(2, 4) = 6P^2 - 8P^3 + 3P^4 \tag{3.28}$$

Figure 3-11 is a plot of the probability of detection or false alarm versus single-dwell P_D or P_{FA}. Note that for typical single-dwell probabilities of detection (i.e., >50%) the cumulative P_D improves (increases), and for low probabilities of false alarm (i.e., <0.2) the cumulative P_{FA} also improves (is decreased). The only "cost" of this improvement is an extended antenna dwell time for each beam position to collect the required data and to conduct n detection tests instead of just one.

To get a better idea of the specific value of the effect of m-of-n detection rules, Table 3-3 presents some specific examples of the effect on P_D, and Table 3-4 presents examples of the effect on P_{FA}. A single-dwell P_D of 0.9 and P_{FA} of 10^{-3} provides 0.996 P_D and $5.92 \times 10^{-4} P_{FA}$ for 2 of 4 scans.

It is sometimes the case that the multiple dwells are not collected on a single scan but rather on successive scans. While this adds significant delay to the data collection

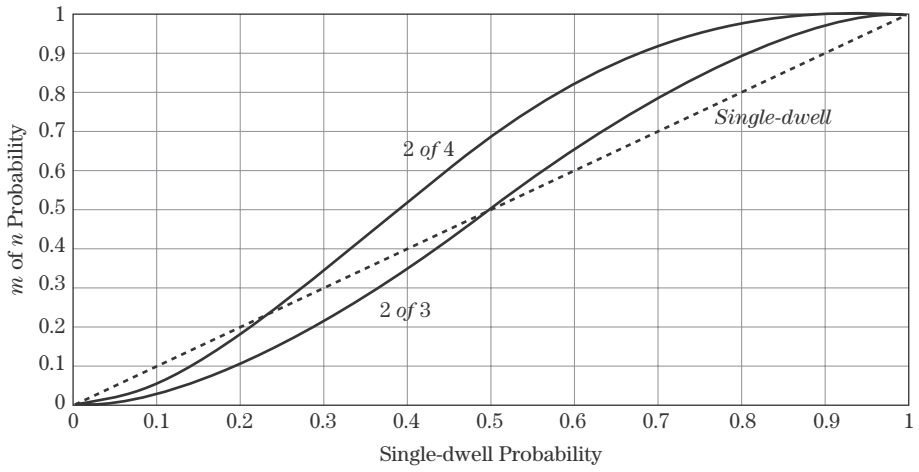

FIGURE 3-11 ■ 2-of-3 and 2-of-4 probability of threshold crossing versus single-dwell probability.

TABLE 3-3 ■ m-of-n Probability of Detection Compared with Single-Dwell Probability of Detection

$P_D(1)$	$P_D(2, 3)$	$P_D(2, 4)$
1	1	1
0.95	0.993	0.999
0.90	0.972	0.996
0.85	0.939	0.988
0.80	0.896	0.973
0.75	0.844	0.949
0.70	0.784	0.916

TABLE 3-4 ■ m-of-n Probability of False Alarm Compared with Single-Dwell Probability of False Alarm

$P_{FA}(1)$	$P_{FA}(2, 3)$	$P_{FA}(2, 4)$
1	1	1
0.1	2.8×10^{-2}	5.23×10^{-2}
0.01	2.98×10^{-4}	5.92×10^{-4}
0.001	2.998×10^{-6}	5.992×10^{-6}
0.0001	2.9998×10^{-8}	5.9992×10^{-8}
0.00001	3.000×10^{-10}	5.9999×10^{-10}

protocol and therefore the time to make a detection decision, for many applications this extra latency in the detection process is acceptable.

Some system applications require even larger numbers of dwells at a given beam position. For example, an airborne pulse Doppler radar typically performs the search function in a high PRF mode to separate moving targets from wide clutter spectral characteristics. Consequently, the radar is highly ambiguous in range, and there is a high likelihood of range eclipsing.[6] Even in the medium PRF mode, there is likely to be range and Doppler aliasing and eclipsing.[7] To improve the P_D and P_{FA} statistics in these conditions, often six or eight dwells are used. Figure 3-12 shows the results of using equation (3.26) to compute the resulting P_D and P_{FA} for 3-of-6 and 3-of-8 detection rules. A single-dwell P_D of 90% results in a processed P_D of very close to 100% for these conditions. In this application, the m-of-n rule is often combined with the use of *staggered PRFs*, discussed in Chapter 17.

The question arises as to whether it is more efficient to use a relatively large number of dwells, which costs significant time, or to increase the single-dwell time. To examine this, consider the following example. Assume a P_D of 95% and a P_{FA} of 10^{-6} is required for each complete scan. For a Swerling 1 target, the single-dwell SNR must be 24.3 dB. Using Figure 3-12, it is seen that, using 3-of-6 processing, a cumulative $P_D = 95\%$ and P_{FA} of 10^{-6} can be achieved if the single-dwell P_D is about 73% and the single dwell P_{FA}

[6] In a pulsed radar, any target that has a range delay exactly equivalent to a multiple of the interpulse period will not be detected because the target echo arrives during a subsequent transmit time. This condition is called *eclipsing*. It can be overcome by changing the pulse interval.

[7] In a coherent radar, the target can be eclipsed in the frequency (Doppler) domain, much like the time domain case already described.

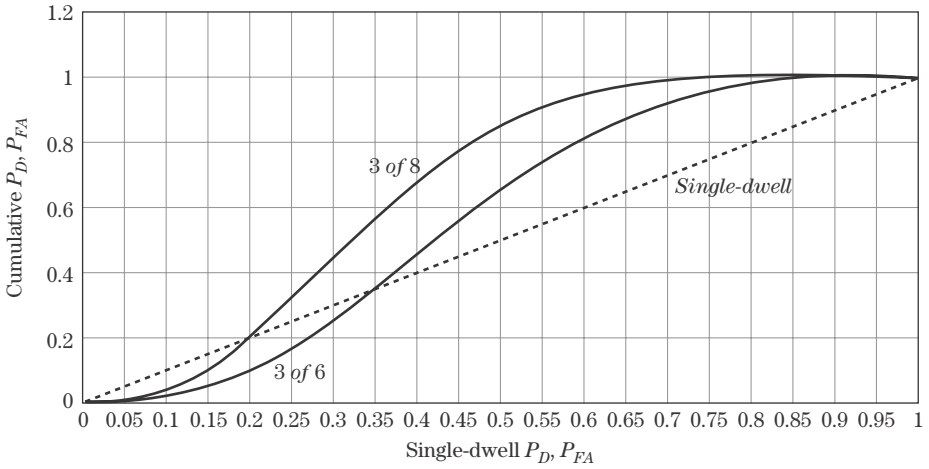

FIGURE 3-12 ■ 3-of-6 and 3-of-8 probability of threshold crossing versus single-dwell probability.

is about 0.001. Using equation (3.23), it is seen that this performance can be obtained with a single-dwell SNR of only 13.2 dB.

This reduction of the required SNR by 11.1 dB (a factor of about 10.4) means that the radar can be "smaller" in some sense by a factor of 10.4. This could take the form of a reduction in average power, antenna gain, single dwell time, or relaxed restrictions on losses. For instance, although six dwells are now required, each one could be shorter by a factor of 10.4, reducing the overall time required to meet the detection specification. Taken a step further, 99% P_D can be achieved with eight dwells and is equivalent to nearly 20 dB of additional radar sensitivity. Extending the time line by a factor of 8 can thus reduce the radar "size" by a factor of 100.

3.4 FURTHER READING

More rigorous mathematical developments of the expressions for P_D and P_{FA}, as well as the general approach of threshold detection, are found in several radar texts [e.g., 3,6,10,20]. These references also extend the results discussed here to the effect of noncoherent integration of multiple samples prior to threshold testing.

Within this volume, target fluctuation models are discussed in more detail in Chapter 7. The application of the detection concepts discussed here to fluctuating target models is discussed in Chapter 15, which also provides both the corresponding exact expressions for P_D and P_{FA} for all of the Swerling models as well as an Albersheim-like approximation.

3.5 REFERENCES

[1] Barton, D.K., *Radar System Analysis*, Artech House, Dedham MA, 1976, Section 1.2.

[2] Rice, S.O., "Mathematical Analysis of Random Noise," *Bell System Technical Journal,* vol. 23, no. 3, July 1944, pp. 282–332; vol. **24**, no. 1, January 1945, pp. 46–156.

[3] DiFranco, J.V., and Rubin, W.L., *Radar Detection*, Artech House, Dedham, MA, 1980, pp. 306–309.

[4] Long, M.W., *Airborne Early Warning System Concepts*, Artech House, Dedham MA, 1992, pp. 498–499.

[5] Farina, A., *Radar Handbook*, 3d ed., *Electronic Counter-Countermeasures*, McGraw-Hill, New York, 2008, Ch. 24.

[6] Barton, D.K., *Modern Radar System Analysis*, Artech House, Norwood, MA, 1988, Section 2.2.

[7] Blake, L.V., *Radar Handbook*, 2d ed., *Prediction of Radar Range,* McGraw-Hill, New York, 1990, Ch. 2.

[8] Skolnik, M.I., *Introduction to Radar Systems*, 3d ed., McGraw Hill, New York, 2001, p. 66.

[9] Nathanson, F.E., *Radar Design Principles*, 2d ed., McGraw-Hill, New York, 1991, pp. 54, 83–86, 89–92.

[10] Meyer, D.P., and Mayer, H.A., *Radar Target Detection, Handbook of Theory and Practice*, Academic Press, New York, 1973.

[11] Sangston, K.J., and Gerlach, K.R., "Coherent Detection of Radar Targets in a Non-Gaussian Background," *IEEE Transactions on Aerospace and Electronic Systems*, vol. 30, no. 2, pp. 330–340, April 1994.

[12] Schleher, D.C., "Radar Detection in Log-Normal Clutter," *Proceedings of the IEEE International Radar Conference,* pp. 262–267, 1975.

[13] Gini.F., Greco, M.V., and Farina, A., "Clairvoyant and Adaptive Signal Detection in Non-Gaussian Clutter: A Data-Dependent Threshold Interpretation," *IEEE Transactions on Signal Processing*, vol. 47, no. 6, pp. 1522–1531, June 1999.

[14] Albersheim, W.J., "Closed-Form Approximation to Robertson's Detection Characteristics," *Proceedings of the IEEE*, vol. 69, no. 7, p. 839, July 1981.

[15] Tufts, D.W., and Cann, A.J., "On Albersheim's Detection Equation," *IEEE Transactions on Aerospace and Electronic Systems*, vol. AES-19, no. 4, pp. 643–646, July 1983.

[16] Shnidman, D.A., "Determination of Required SNR Values," *IEEE Transactions on Aerospace & Electronic Systems*, vol. AES38, no. 3, pp. 1059–1064, July 2002.

[17] Richards, M.A., *Fundamentals of Radar Signal Processing*, McGraw-Hill, New York, 2005.

[18] Bulmer, M.G., *Principles of Statistics*, Dover Publications, New York, New York, 1967, p. 84.

[19] Barton, D.K., Cook, C.E., and Hamilton, P., *Radar Evaluation Handbook,* Artech House, Dedham, MA, 1991, pp. 4–17.

[20] Minkler, G., and Minkler, J., *CFAR, The Principles of Automatic Radar Detection in Clutter,* Magellan Book Co., Baltimore, MD, 1990.

3.6 PROBLEMS

1. For a mechanically scanned antenna having an azimuth beamwidth of 2 degrees and an elevation beamwidth of 3 degrees, how many beam positions are required to search a volume defined by a 90 degree azimuth sector and a 6 degree elevation sector?

2. If the antenna were raster scanning at 180 degrees per second (i.e., it is scanning in azimuth at 180 degrees per second), what is the maximum dwell time for each beam position? Assume it takes no time to change to a new elevation position and azimuth scanning direction.

3. For the previous conditions, what is the total frame search time?

4. For a phased array antenna, suppose the beamwidth at array normal is 2 degrees by 3 degrees (same as in problem 1). Also suppose that the dwell time used for scan angles between 0 and ±30 degree is 4 msec, while for scan angles between ±30 and ±45 degrees it is 6 msec. If the beam position is stepped in equal step sizes, what is the total search frame time? Assume it takes negligible time to move from one position to the next.
5. What is the P_{FA} if the threshold voltage is set at three times the root mean square (rms) noise voltage?
6. What threshold voltage is required to effect a P_{FA} of 10^{-4} if the rms noise voltage is 150 mv?
7. Assuming $P_{FA} = 10^{-4}$, how many consecutive verifications are required to effect a P_{FA} of 10^{-9} or less?
8. For a search volume that requires: 45 beam positions, 333 range bins, 32 Doppler bins, and a P_{FA} of 5×10^{-5}, how many false alarms occur on average in a single search frame?
9. Consider a weapon locating radar having a beamwidth of 2 degrees in both azimuth and elevation that is set up to search a volume defined by a 75 degree sector in azimuth and a 4 degree sector in elevation. If the radar also has a dwell time of 2.4 msec and a plan to spend 5 dwells at each beam location, what is the total scan time?
10. If there are eight targets being tracked by the system in problem 9, each consuming 6 milliseconds per track update at an update rate of 10 Hz (10 updates per second), what is the new search scan time?
11. Your enemy, 20 km distant, fires a mortar round in your general direction. The round has a vertical component of velocity of 200 meters per second. (Assume that this does not change during the search time.) You are searching the area using a weapon-locating radar. What must your maximum scan time be to ensure at least four opportunities to detect the target before it passes through your "search fence," which is the elevation sector extending from 0 to 4 degrees above the horizon?
12. If the round in problem 11 is detected at 2 degrees above the horizon, what must the track sample rate be to get 50 track samples from between the point of detection and an elevation of 6 degrees above the horizon?
13. Given a radar system that has a single-dwell P_D of 50% and a single-dwell P_{FA} of 5×10^{-3}, what are the cumulative P_D and P_{FA} for 2-of-3 and 2-of-4 multiple-dwell processes?
14. For a radar system that has a single-dwell P_D of 75% and a single-dwell P_{FA} of 5×10^{-3}, what are the P_D and P_{FA} for 2-of-3 and 2-of-4 multiple-dwell processes?
15. Assuming that the target exhibits Swerling 1 fluctuations and that the P_D and P_{FA} that result from the multidwell (2-of-4) processing in problem 14 are adequate, what SNR improvement is required to provide the same P_D and P_{FA} in a single dwell?
16. Suppose a phased array search radar has to complete searching a volume defined by 10 degrees in azimuth, 10 degrees in elevation, and 40 km in range in 0.62 seconds. The range resolution is 150 meters, obtained with a simple 1 microsecond pulse width. At the center of the search sector, the antenna has a 2.7 degree azimuth beamwidth and a 2.7 degree elevation beamwidth. Since the target for which the system is searching is a moving target and there is surface clutter interfering with the detection, Doppler processing is used. There are 64 Doppler bins developed by the FFT processor. During a single search pattern, it is required that the probability of detecting a target is 99%, and on average one false alarm is allowed. What is the resulting P_D and P_{FA} if the single-dwell P_D is 90% and the single-dwell P_{FA} is 0.01? If 3-of-5 processing is employed, do the resulting P_D and P_{FA} meet the requirements?